

1 Atypical nighttime spread-F structure observed near the southern crest of the
2 ionospheric equatorial ionization anomaly

3

4 Fagundes¹ PR, Bittencourt² JA, de Abreu¹ AJ, Moor¹ LP, Muella¹ MTAH, Sahai¹
5 Y, Abalde¹ JR, Pezzopane³ M, Sobral² JHA, Abdu² MA, Pimenta² AA, Amorim²
6 DCM

7

8 1-Física & Astronomia, Universidade do Vale do Paraíba (UNIVAP), Avenida
9 Shishima Hifumi, 2911, Sao Jose dos Campos, SP, Brazil.

10 2- Instituto Nacional de Pesquisas Espaciais (INPE), Sao Jose dos Campos,
11 SP, Brazil.

12 3- Istituto Nazionale di Geofisica e Vulcanologia, Via di Vigna Murata 605,
13 00143, Rome, Italy.

14

15 **Abstract**

16 An atypical nighttime spread-F structure is observed at or above the F-layer,
17 near the crest of the ionospheric equatorial ionization anomaly region (EIA).
18 This ionospheric atypical spread-F phenomenon was observed using two
19 closed spaced (~115 km) ionospheric soundings stations located in Sao Jose
20 dos Campos (23.21°S, 45.97°W) and Cachoeira Paulista (22.70°S, 45.01°W),
21 Brazil, in a low-latitude station (near the southern crest of the EIA region),
22 during nighttime, low solar activity, and quiet geomagnetic conditions. This
23 structure, in the initial phase, appears as a faint spread-F trace above or at the
24 F2-layer peak height. After a few minutes, it develops into a strong spread-F
25 trace, and afterwards, it moves to altitudes below to the F2-layer peak heights.

26 Finally, the atypical nighttime F-layer trace structure may remain for a while
27 between the F-layer bottom side and peak height or can move to an altitude
28 above the F-layer peak height, and then it disappears. In order to have a
29 comprehensive view of the ionospheric environment characterizing the
30 phenomenon under study, complementary GPS data were used to investigate
31 the ionosphere environment conditions, during both events. The 6 GPS stations
32 used in this study are distributed from near the equatorial region to low
33 latitudes.

34

35

36 **1- Introduction**

37 Several F-layer phenomena at equatorial and low-latitude regions have
38 attracted considerable interest of different investigating groups for over fifty
39 years. Among these phenomena, spread-F, zonal electric field pre-reversal
40 enhancement (PRE), equatorial ionospheric anomaly (EIA), and F3-layer
41 formation have been studied by numerous researchers. Nevertheless, these
42 topics are still attracting much attention, particularly studies related to the day-
43 to-day variability of these phenomena. In this paper, we report the occurrence of
44 an atypical nighttime structure at or above the F2-layer, near the southern crest
45 of the EIA (low latitude).

46

47 The ionospheric vertical electron density profile can be modified
48 continuously by waves, chemistry, solar radiation, and solar activity. However,
49 the main vertical features of the D, E, F1, and F2 layers are usually identifiable,
50 except during strong geomagnetic storms. During daytime, the various

51 ionospheric layers are normally present. During nighttime the D and F1 layers
52 disappear, while the E layer takes some time to disappear, and, finally, only the
53 F2-layer remains. Both theoretical and observational investigations, related to
54 the day-to-day variability of the F-layer in equatorial and low-latitude regions,
55 have become very active research subjects (Fagundes et al., 1999, 2009a,
56 2009b; Paul and DasGupta 2010; Tsunoda, 2010). The equatorial spread-F
57 (ESF) phenomenon is one of the most studied topics. The onset conditions and
58 the possible causes for the day-to-day ESF variability are hot topics in this
59 research area (Abdu et al., 1982 and Sastri et al., 1997). Therefore, the
60 knowledge related to ESF latitudinal and longitudinal morphology, seasonal and
61 solar cycle variations for each longitudinal sector (American, Asian, and Indian),
62 and zonal drift speeds has increased considerably during the last decade
63 (Abalde et al., 2001; Bittencourt et al., 1997; Fagundes et al., 1995; Pimenta et
64 al., 2001, 2003; Sahai et al., 2004, 2009, Sobral et al., 1999, 2011). Calvert and
65 Cohen (1961) investigated some characteristics of spread echoes, at equatorial
66 region, on ionograms and conclude that its main feature depend on (a) nature of
67 the scattering irregularities and (b) the distribution of them in the east-west
68 plane with respect to the ionosonde. In fact, by taking into account appropriate
69 distribution of scattering centers in the east-west plane, they succeeded in
70 simulating several features of the observed ESF signatures.

71

72 F3-layer formation and its day-to-day variability at equatorial and low
73 latitudes is another topic that has become very active in the last decades. The
74 F3-layer is characterized by the formation of an additional electron density peak
75 above the F2-layer peak. Seasonal and solar cycle variations, their possible

76 sources, and occurrence during geomagnetically quiet and disturbed periods
77 are the primary subjects explored related to the F3-layer (Abdu et al., 1992,
78 Balan and Bailey, 1995; Balan et al., 1997, 1998, 2008; Batista et al., 2002,
79 2003; Depuev and Pulinets, 2001; Jenkins et al., 1997; Lynn et al., 2000;
80 Pulinets et al., 2002; Uemoto et al., 2006; Fagundes et al., 2007, 2011;
81 Paznukhov et al., 2007; Rama Rao et al., 2005, Zain et al., 2008; Sreeja et al.,
82 2009, 2010, Zhao et al., 2009, Klimenko et al., 2011). Near the equatorial
83 region, F3-layer formation can be explained by the combined effects of a large
84 $\mathbf{E} \times \mathbf{B}$ drift, during the morning period, which uplifts the F2-layer around the
85 magnetic equator, and a meridional wind flowing from the summer hemisphere
86 to the winter hemisphere, which acts to raise the plasma in the summer
87 hemisphere. However, the meridional wind near the magnetic equator has a
88 smaller vertical component than at a few degrees of latitude away from the
89 magnetic equator, and, consequently, the F3-layer is weaker at the magnetic
90 equator and stronger a few degrees away from it (Jenkins et al., 1997).
91 Nevertheless, this mechanism based on the combined effects of $\mathbf{E} \times \mathbf{B}$ drift and
92 meridional wind, proposed by Balan et al.(1997, 1998) for the equatorial region,
93 does not explain F3-layer formation near the southern crest of the equatorial
94 ionospheric anomaly (EIA) in the American sector (Fagundes et al., 2007 and
95 2011). Therefore, based on observations, Fagundes et al. (2007) proposed that
96 medium scale traveling ionospheric disturbances (MSTIDs), generated by
97 gravity waves (GWs), can play an important role in F3/F2-layer stratification in
98 the regions near the EIA crests.
99

100 In this paper, we present and discuss two nighttime atypical spread-F
101 events similar to those observed by [Calvert and Cohen \(1961\)](#) at equatorial
102 region, but the present observations were carried out in Sao Jose dos Campos
103 (23.21°S, 45.97°W) and in Cachoeira Paulista (22.70°S, 45.01°W), Brazil, in a
104 low-latitude station (near the southern crest of the ionospheric equatorial
105 ionization anomaly - EIA). The most interesting feature of this atypical F-layer
106 structure is their time evolution. In the initial phase it appears as a weak spread-
107 F at or above the F-layer trace peak height. Afterwards, the spread-F trace
108 structure strengthens and moves to heights below the F-layer trace peak
109 heights. Finally, this atypical structure shows electron density values larger than
110 those of the F-layer and then disappears. Also, GPS data of six stations were
111 used to investigate the ionospheric environment along the meridional direction
112 from near equatorial region to low latitude and over the two ionosonde stations.
113 Figure 1 shows a map indicating the geographical position of the ionosondes
114 and GPS stations used in this work.

115

116 **2- Observations and Results**

117 Spread-F at equatorial and low-latitudes regions is a well-known
118 phenomenon and is closely related to large-scale equatorial spread-F or plasma
119 bubbles, associated with range spread-F signatures on the ionograms
120 ([Fagundes et al., 1999](#), [Abalde et al., 2001](#)). Also, in the equatorial and low-
121 latitudes regions a second class of spread-F is observed, called frequency
122 spread-F. Nevertheless, the observed spread-F phenomenon described in this
123 investigation seems to be unrelated to large-scale equatorial irregularities. This
124 ionospheric atypical spread-F phenomenon was observed from ionospheric

125 soundings carried out in Sao Jose dos Campos (23.21°S, 45.97°W; hereafter
126 referred to as SJC) and Cachoeira Paulista (22.70°S, 45.01°W; hereafter
127 referred to as CP), Brazil, in a low-latitude station, two closed-spaced low-
128 latitude stations (~115 km), near the southern crest of the EIA region, during
129 nighttime, in geomagnetically quiet conditions, and low solar activity (Figures 2,
130 3, 4 and 5). These two closed spaced ionospheric stations (SJC and CP) are
131 separated by ~0.5° (57 km) in latitude and ~1° (99 km) in longitude. Therefore,
132 ionograms recorded almost simultaneously in these two stations, must have
133 very similar traces. However, if small-scale irregularities propagate at
134 ionospheric heights, in this region, then the ionogram traces observed in both
135 sites will show differences. On the other hand, if large-scale ionospheric
136 irregularities, with dimension of hundred kilometers, propagate over this region,
137 it will be very difficult to notice any significant difference in the ionogram traces,
138 in both sites. Therefore, these two closed spaced ionosonde stations have a
139 good configuration to study small-scale structures propagating around these
140 sites.

141

142 The six GPS data used in this work were obtained using the following
143 receiving stations: Palmas (PAL), Brasilia (BRA), Rio Paranaiba (RPA), Rio de
144 Janeiro (RIO), Ourinhos (OUR) and, Sao Jose dos Campos (SJC). These GPS
145 stations are located from near the magnetic equatorial to the crest of the EIA
146 region and over SJC and CP ionosonde stations. Figure 1 and Table 1 provide
147 full details of the GPS receivers and the ionosonde stations considered in the
148 present work. The GPS observations were used to obtain the rate of change of
149 TEC, called ROT, this parameter is very useful to identify the presence of

150 ionospheric irregularities ([Aarons et al. 1997](#)). The presence or absence of
151 large-scale irregularities, around a specific station, show very clear signature in
152 the ROT signals (see Figure 6). On the contrary, the presence of small-scale
153 irregularities is more difficult to be observed by means of change of TEC (ROT
154 parameter).

155

156 Figures 2, 3, 4, and 5 show step by step the development of the events
157 observed on March 13, 2010 and March 19, 2010, in SJC and CP. Initially, the
158 F2-layer presents its usual behavior after a weak post-sunset uplift, if this is
159 compared with those characterizing days of "fresh spread-F" occurrence,
160 probably associated with a small electric field pre-reversal enhancement (for
161 more details about "fresh spread-F" see [Fagundes et al., 2009a and 2009b](#)).
162 The ordinary and extraordinary traces are clear on the ionograms and the foF2
163 critical frequency varies from 4 to 6 MHz. However, slightly above the F2-layer
164 peak height trace, a small spread-F structure trace appears, with frequencies
165 that are higher than the F2-layer critical frequency (foF2). In the initial stage,
166 this structure is faint and, apparently, not related with the F2-layer trace.
167 However, after a few minutes, the structure trace becomes stronger and shows
168 spread-F characteristics. Then the structure trace moves to heights between the
169 bottom side and the peak of the F2-layer trace and turns into an atypical F-layer
170 structure trace.

171

172 The four phases characterizing the nighttime atypical spread-F trace
173 structure time evolution, that took place on March 13, 2010, are presented in
174 Figures 2 and 3, for SJC and CP, respectively. The observed atypical

175 phenomenon is very dynamical and changes rapidly its characteristics in a time
176 scale of a few minutes. Figure 2A shows an ionogram with the first stage of the
177 nighttime atypical spread-F trace structure in SJC at 03:05 UT (00:05 LT). The
178 first echoes of this structure span between 530 km and 610 km in virtual height
179 and range from 5.9 to 7.7 MHz. At this stage, in SJC, it is not clear if these
180 echoes belong to an atypical F-layer trace structure. The ionogram observed at
181 03:07 UT (00:07LT) in CP does not show any evidence of this atypical spread-F
182 trace structure, despite of the fact that these two sites are separated only ~115
183 km (Figure 3A). However, the first stage of the atypical spread-F trace structure
184 appeared in CP only at 03:15 UT (00:15 LT - Figure 3B), indicating that the
185 early stage of the spread-F trace structure appears in CP only 10 minutes later
186 than in SJC. On the other hand at 03:10 UT (00:10 LT) in SJC (Figure 2B), the
187 nighttime atypical spread-F trace structure becomes stronger and appears very
188 clearly in the ionogram, with many more echoes. At this stage, the spread-F
189 trace structure is well-developed above or at the F2-layer peak height, with
190 frequencies higher than foF2, and there is a gap between the F2 critical
191 frequency (foF2) and the range-type spread-F trace structure minimum echo
192 frequencies. Again, a few minutes later, the atypical spread-F trace structure
193 becomes stronger in CP (Figure 3C, 03:22 UT (00:22 LT)), but this ionogram
194 shows both, a spread-F structure and satellite traces. By then, the spread-F
195 trace structure has already become a satellite trace of the F2-layer in SJC at
196 03:20 UT (00:20 LT - Figure 2C). The F2-layer trace does not show spread-F
197 trace occurrence and, on the other hand, the satellite trace (related to the
198 spread-F structure) changes from range to frequency spread-F and presents a
199 larger critical frequency than the F2-layer. A similar ionogram is observed in CP

200 at 03:37 UT (00:37 LT - Figure 3D). Finally, Figure 2D (SJC) shows an
201 ionogram recorded at 03:40 UT (00:40 LT), where the satellite traces (related to
202 spread-F trace structure) and the F2-layer trace are seen to be much closer to
203 each other.

204

205 Figures 4 and 5 show four phases of another similar atypical spread-F
206 trace structure observed in SJC and CP on March 19, 2010. In the beginning of
207 this event, the ordinary and extraordinary F2-layer traces appear very clearly on
208 the ionograms, in SJC at 00:55 UT (21:55 LT). Again, the initial phase of the
209 atypical structure trace initiates with a few spread-F echoes (Figure 4A), such
210 as range spread-F trace, but these echoes appear above or at the F2-layer
211 peak height trace and have frequencies between 5.0 to 5.5 MHz, which are
212 higher than foF2 (3.4 MHz). In this initial stage, (00:55 UT - 21:55 LT) it is not
213 clear whether these echoes belong to F-layer structure. It is important note that
214 also for this event the initial stage in CP appear 20 minutes later than in SJC, at
215 01:15 UT (22:15 LT) and remain until 01:22 (22:22 LT) (Figures 5A and 5B). A
216 few minutes later in SJC (01:05 UT - 22:05 LT) or in the second phase, ordinary
217 and extraordinary of the F2-layer traces remain clear on the ionograms (Figure
218 4B), but the spread-F trace structure is well developed. Nevertheless, the
219 spread-F trace structure is well separated from the F2-layer trace. The
220 frequency gap between the F2-layer critical frequency (foF2) and the first
221 echoes of the spread-F trace structure is also in this case significant. Figure 4C
222 and 5C show the third phase of the event at 01:55 UT (22:55 LT) and 01:52 UT
223 (22:52 LT) for SJC and CP, respectively. The ordinary and extraordinary traces
224 of the F2-layer are still clear, and only the atypical structure present spread-F.

225 However, this atypical spread-F trace structure merges with the F2-layer, close
226 to the F2 peak height. The last phase of the phenomenon under study is shown
227 in Figures 4D and 5D, in which the atypical spread-F trace structure starts
228 moving upward and appears much more separated from the F2-layer trace.
229 Finally, the structure disappears and the F2-layer recovers its normal
230 characteristics. A sequence of ionograms, as a movie, for SJC and CP can be
231 seen in the supplementary material, showing the time evolution of both events
232 described in this paper. The time resolutions of ionograms are 5 minutes and 8
233 minutes for SJC and CP, respectively.

234

235 The rate of change of TEC (ROT) plots shown in Figure 6 for Mach 13
236 and 19, 2010 indicate that equatorial irregularities were generated during these
237 nights, but were confined to equator and regions close by, as seen by the rapid
238 and large ROT variations, recorded in PAL and BRA between 00:00 UT (21:00
239 LT) and 04:00 UT (01:00 LT) by most of satellites, black rectangle in Figures 6A
240 and 6B). The ROT recorded at RPA shows some evidence that the irregularities
241 formed at equator reached latitudes between BRA and RPA on March 13,
242 because, even though smaller, some satellites show ROT variation, green
243 rectangle, in Figures 6A and 6B. On the contrary, the ROT recorded in RIO for
244 both days, does not show any signature of equatorial irregularities.

245

246 Nevertheless, the presence of small-scale structure was observed in ORI
247 and SJC, on March 13 (Figure 6), at the same time for which the atypical
248 spread-F structure under study was observed by ionosonde in SJC and CP. It is
249 important to highlight that this structure must be small, because only the

250 satellites 3 and 19 detect the structure in ORI and satellite 19 in SJC (red
251 rectangle, Figures 6A and 6B).

252

253 On the other hand, the atypical structure that was observed on March 19
254 by the ionosondes was probably even much tinier, because the ROT recorded
255 in ORI shows a very small and short change amplitude variation (red rectangle,
256 Figure 6B). But, the ROT in RPA, RIO and, SJC did not show ROT variation.

257

258 **3- Discussion and Conclusions**

259

260 Calvert and Cohen (1961) by observing atypical ionograms in Huancayo,
261 at the magnetic equator, noticed atypical spread-F trace signatures similar to
262 those we illustrated in this paper. Unlike Calvert and Cohen (1961), the events
263 described in this work were observed at low-latitudes, near the southern crest of
264 the EIA. They mentioned that the observed irregularities were apparently
265 anomalous and are more closely related to spread-F observed at mid-latitudes
266 than the equatorial spread-F and used the ray traced technique and concluded
267 that the anomalous traces on the ionograms were generated by irregularities
268 away from the overhead ionosonde site. However, in their paper they do not
269 discuss the possible generation sources for this kind of structure.

270

271 The atypical spread-F structure investigated in this paper at low-latitudes
272 is not related to the large-scale irregularities coming from the equator. On the
273 other hand, recently propagation of GWs and MSTIDs has been suggested as a
274 possible source of F2-layer stratification and spread-F signatures at low-

275 latitudes in the Brazilian sector. [Abdu et al. \(1982\)](#) proposed that stratification of
276 the nighttime F2-layer, during the pre-sunrise period, over CP, is due to the
277 passage of GWs. [Pimenta et al. \(2008\)](#), using a ground-based all-sky imaging
278 system in CP, observed dark band structures (MSTIDs) propagating from
279 southeast to northwest. These optical measurements showed that the MSTIDs
280 move quasi-horizontally through the ionosphere and that they are frontal in
281 nature. [Amorim et al. \(2011\)](#) evidenced the occurrence of spread-F at the same
282 time that the all-sky images registered MSTIDs over the zenith of CP, and they
283 found that both the peak height and the virtual height ionospheric parameters
284 registered abrupt uplifting. [Makela et al. \(2010\)](#) observed interesting airglow OI
285 630 nm band structures extending from low-latitude to near-equatorial regions
286 (type MSTID), propagating towards the northwest, during a deep low solar
287 activity period. All these observations show that the presence of MSTIDs, at low
288 latitudes, is a very common feature and can be a source irregularities causing
289 spread-F signatures on the ionograms.

290

291 Both cases presented in this investigation are very interesting examples
292 of an ionospheric structure developing at or above the F2-layer. The time
293 evolution of the atypical nighttime spread-F structure reinforces the idea that
294 ionization transport processes related to MSTIDs, propagating at low latitudes,
295 may be a source for generating the F2-layer stratification or F3-layer ([Abdu et](#)
296 [al., 1982](#), [Fagundes et al., 2007](#)). However, the cases illustrated in this work
297 suggest that MSTIDs, in the initial phase, must have a strong horizontal
298 component, as compared to the vertical component, and propagate just above
299 or at the F2-layer peak height. In this case, it seems that the MSTIDS were able

300 to construct a situation that caused spread-F formation. However, the spread-F
301 was generated above the F2-layer peak height, which is very different from the
302 large-scale spread-F that is usually generated near the F-layer bottom side.
303 Another aspect to be considered is that this phenomenon may be somewhat
304 related to the deep low solar activity period that took place in 2010.

305

306 The occurrence of an atypical spread-F structure at low latitudes is
307 reported. The occurrence of this atypical phenomenon can be subdivided into
308 four stages: 1) A faint structure is seen as a few echoes above the F2-layer in
309 ionograms; 2) The structure becomes stronger and evolves into spread-F
310 characteristics; but it is still not connected with the F2-layer; 3) The structure
311 merges with the F2-layer and becomes an atypical spread-F; and 4) The
312 atypical spread-F disconnects from the F2-layer and disappears, or it merges
313 with the F2-layer and disappears. It is important mention that the structure was
314 observed simultaneously by GPS ROT variation despite the GPS technique is
315 good for to observe larger structures and during moderate-high solar activity,
316 when the total electron content (TEC) is larger.

317

318 In this paper, we presented what appears to be another ionogram
319 signature of MSTIDs propagating above or at F2-layer peak that generates an
320 extra ionospheric structure just above or at the F2-layer, during nighttime, at low
321 latitudes. The observation characteristics of this atypical nighttime spread-F
322 trace structure indicate that some unknown or not well-understood generation
323 mechanisms may be involved at equatorial and low-latitude regions. Also, the
324 structure, in both occasions, is observed first at SJC and after a few minutes at

325 CP, suggesting that the structure propagates towards northeast. But, to
326 determine the structure direction and speed velocity it is needed at least three
327 ionosonde closed spaced. The GPS ROT data suggests that this structure is
328 located around the two closed spaced ionosonde stations. Therefore,
329 coordinated observations from multi-sites and multi-instruments (optical and
330 radio) are relevant and important to understand the features of this kind of
331 structure.

332

333 **4- References**

334

335 Aarons, J., M. Mendillo, and R. Yantosca GPS phase fluctuations in the
336 equatorial region during sunspot minimum, *Radio Sci.*, 32, 1535–1550,
337 doi:10.1029/97RS00664, 1997.

338 Abalde JR, Fagundes PR, Bittencourt JA, Sahai Y Observations of equatorial F
339 region plasma bubbles using simultaneous OI 777.4 nm and OI 630.0 nm
340 imaging: New results. *J. Geophys. Res.*, 106 (A12), 30331-30336, 2001.

341 Abdu MA, Batista IS, Kantor IJ, Sobral JHA Gravity wave induced ionization
342 layers in the night F-region over Cachoeira Paulista (22°S, 45°W). *J. Atmos.*
343 *Solar Terr. Phys.*, 44(9), 759-767, 1982.

344 Abdu, M. A.; Medeiros, R. T.; Sobral, J. H. A. Equatorial Spread-F Instability
345 Conditions as Determined from Ionograms. *Geophys. Res. Lett.*, 9(6), 692-
346 695, 1982.

347 Abdu, M. A.; Batista, I. S.; Sobral, J. H. A. A New Aspect of Magnetic
348 Declination Control on Equatorial Spread-F and F-Region Dynamo. *J.*
349 *Geophys. Res.*, 97(10), 14897-14904, 1992.

350 Amorim DCM, Pimenta AA, Bittencourt JA, Fagundes PR Long-term study of
351 medium-scale traveling ionospheric disturbances using O I 630 nm all-sky
352 imaging and ionosonde over Brazilian low latitudes.
353 doi:10.1029/2010JA016090, J. Geophys. Res., 2011.

354 Balan N and Bailey GJ Equatorial plasma fountain and its effects: Possibility of
355 an additional layer. J. Geophys. Res., 100 (A11), 21421-21432, 1995.

356 Balan N, Bailey GJ, Abdu MA, Oyama KI, Richards PG, MacDougall J, and
357 Batista IS Equatorial plasma fountain and its effects over three locations:
358 Evidence for an additional layer, the F3 layer. J. Geophys. Res., 102 (A2),
359 2047-2056, 1997.

360 Balan N, Batista IS, Abdu MA, MacDougall J, Bailey GJ Physical mechanism
361 and statistics of occurrence of an additional layer in the equatorial
362 ionosphere. J. Geophys. Res., 103, (A12), 29169-29181, 1998.

363 Balan N, Thampi SV, Lynn K, Otsuka Y, Alleyne H, Watanabe S, Abdu MA,
364 Fejer BG F-3 layer during penetration electric field. J. Geophys. Res., 113,
365 A00A07, DOI: 10.1029/2008JA013206, 2008.

366 Batista IS, Abdu MA, MacDougall J, Souza JR Long term trends in the
367 frequency of occurrence of the F3 layer over Fortaleza, Brazil. J. Atmos.
368 Solar Terr. Phys., 64, 1409–1412, 2002.

369 Batista IS, Abdu MA, da Silva AM, and Souza JR Ionospheric F3 Layer:
370 Implications for the IRI Model. Adv. Space Res., 31(3), 607-611, doi:
371 10.1016/S 0273-1177(03)00023-1, 2003.

372 Bittencourt, JA; Sahai, Y; Fagundes, PR; Takahashi, H Simultaneous
373 observations of equatorial F-region plasma depletions and thermospheric
374 winds. J. Atmos. Solar Terr. Phys., 59 (9), 1049-1059, 1997.

375 Calvert W and Cohen R The interpretation and synthesis of certain Spread-F
376 configurations appearing on Equatorial ionograms. J. Geophys. Res., 66(10),
377 3125-3140, 1961.

378 Depuev, VH, and Pulinets SA Intercosmos-19 observations of an additional
379 topside ionization layer: The F3 layer, Adv. Space Res., 27(6– 7), 1289–
380 1292, 2001.

381 Fagundes, PR; Sahai, Y; Bittencourt, JA; Takahashi, H Relationship between
382 generation of equatorial F-region plasma bubbles and thermospheric
383 dynamics. Adv. Space Res., 16 (5), 117-120, 1995.

384 Fagundes, PR; Sahai, Y; Batista, IS; Abdu, MA; Bittencourt, JA; Takahashi, H
385 Observations of day-to-day variability in precursor signatures to equatorial F-
386 region plasma depletions. Ann. Geophys., 17 (8), 1053-1063, 1999.

387 Fagundes, PR; Klausner, V; Sahai, Y; Pillat, VG; Becker-Guedes, F; Bertoni,
388 FCP; Bolzan, MJA; Abalde, JR Observations of daytime F2-layer stratification
389 under the southern crest of the equatorial ionization anomaly region. J.
390 Geophys. Res., 112 (A4) Art. No. A04302, DOI: 10.1029/2006JA011888,
391 2007.

392 Fagundes, PR; Bittencourt, JA; Abalde, JR; Sahai, Y; Bolzan, MJA; Pillat, VG;
393 Lima, WLC F layer postsunset height rise due to electric field prereversal
394 enhancement: 1. Traveling planetary wave ionospheric disturbance effects. J.
395 Geophys. Res., 114 Art. No. A12321, DOI: 10.1029/2009JA014390, 2009a.

396 Fagundes, PR; Abalde, JR; Bittencourt, JA; Sahai, Y; Francisco, RG; Pillat, VG;
397 Lima, WLC F-layer postsunset height rise due to electric field prereversal
398 enhancement: 2. Traveling planetary wave ionospheric disturbances and

399 their role on the generation of equatorial spread F. *J. Geophys. Res.*, 114 Art.
400 No. A12322, DOI: 10.1029/2009JA014482, 2009b.

401 Fagundes PR, Klausner V, Bittencourt JA, Sahai Y, and Abalde JR Seasonal
402 and solar cycle dependence of F3-layer near the southern crest of the
403 equatorial ionospheric anomaly. *Adv. Space Res.*,
404 DOI:10.1016/j.asr.2011.04.003, 2011.

405 Jenkins, B., G. J. Bailey, M. A. Abdu, I. S. Batista, and N. Balan Observations
406 and model calculations of an additional layer in the topside ionosphere above
407 Fortaleza, Brazil, *Ann. Geophys.*, 15, 753–759, 1997.

408 Klimenko, M.V., Klimenko, V.V., Ratovsky, K.G., Goncharenko, L.P., Sahai, Y.,
409 Fagundes, P.R., de Jesus, R., de Abreu, A.J., Vesnin, A.M. Numerical
410 modeling of ionospheric effects in the middle and low-latitude F-region during
411 geomagnetic storm sequence of September 9–14, 2005. *Radio Sci.* 46, 2011.

412 Lynn KJW, Harris TJ, and Sjarifudin M Stratification of the F2 layer observed in
413 Southeast Asia, *J. Geophys. Res.*, 105(A12), 27147– 27156, 2000.

414 Makela JJ, Miller ES, and Talaat ER Nighttime medium- scale traveling
415 ionospheric disturbances at low geomagnetic latitudes. *Geophys. Res. Lett.*,
416 37, L24104, doi:10.1029/2010GL045922, 2010.

417 Paul, A; DasGupta, A Characteristics of the equatorial ionization anomaly in
418 relation to the day-to-day variability of ionospheric irregularities around the
419 postsunset period. *Radio Sci.*, 45 Art. No. RS6001, DOI:
420 10.1029/2009RS004329, 2010.

421 Paznukhov VV, Reinisch BW, Song P, Huang X, Bullett TW, (Bullett, T. W.);
422 Vellz O Formation of an F3 layer in the equatorial ionosphere: A result from

423 strong IMF changes. *J. Atmos. Solar Terr. Phys.*, 69 (10-11), 1292-1304,
424 DOI: 10.1016/j.jastp.2006.08.019, 2007.

425 Pimenta, AA; Fagundes, PR; Bittencourt, JA; Sahai, Y, Clemesha, B Relevant
426 aspects of equatorial plasma bubbles under different solar activity conditions.
427 *Adv. Space Res.*, 27 (6/7), 1213-1218 2001.

428 Pimenta, AA; Bittencourt, JA; Fagundes, PR; Sahai, Y; Buriti, RA; Takahashi, H;
429 Taylor, MJ Ionospheric plasma bubble zonal drifts over the tropical region: a
430 study using OI 630nm emission all-sky images. *J. Atmos. Solar Terr. Phys.*,
431 65 (10), 1117-1126, DOI: 10.1016/S1364-6826(03)00149-4, 2003.

432 Pimenta, AA; Kelley, MC; Sahai, Y; Bittencourt, JA; Fagundes, PR
433 Thermospheric dark band structures observed in all-sky OI 630 nm emission
434 images over the Brazilian low-latitude sector. *J. Geophys. Res.*, 113 (A1) Art.
435 No. A01307, DOI: 10.1029/2007JA012444, 2008.

436 Pulinets SA, Depuev VH, Karpachev AT, Radicella SM, and Damilkin NP
437 Recent advances in topside profile modeling. *Adv. Space Res.*, 29(6), 815–
438 823, 2002.

439 Rama Rao PVS, Niranjana K, Prasad DSVVD, and Brahmanandam PS Features
440 of additional stratification in ionospheric F2 layer observed for half a solar
441 cycle over Indian low latitudes, *J. Geophys. Res.*, 110, A04307,
442 doi:10.1029/2004JA010646, 2005.

443 Sahai, Y; Fagundes, PR; Abalde, JR; Pimenta, AA; Bittencourt, JA; Otsuka, Y;
444 Rios, VH Generation of large-scale equatorial F-region plasma depletions
445 during low range spread-F season. *Ann. Geophys.*, 22 (1), 15-23, 2004.

446 Sahai, Y; Becker-Guedes, F; Fagundes, PR; de Abreu, AJ; de Jesus, R; Pillat,
447 VG; Abalde, JR; Martinis, CR; Brunini, C; Gende, M; Huang, CS; Pi, X; Lima,

448 WLC; Bittencourt, JA; Otsuka, Y Observations of the F-region ionospheric
449 irregularities in the South American sector during the October 2003
450 'Halloween Storms'. Ann. Geophys., 27 (12), 4463-4477, 2009.

451 Sreeja V, Balan N, Ravindran S, Pant TK, Sridharan R and Bailey GJ Additional
452 stratifications in the equatorial F region at dawn and dusk during
453 geomagnetic storms: Role of electrodynamics. J. Geophys. Res., 14
454 (A08309), doi:10.1029/2009JA014373, 2009.

455 Sreeja V, Ravindran S, Pant TK Features of F3 layer occurrence over the
456 equatorial location of Trivandrum. Ann. Geophys, 28, 1741-1747, 2010.

457 Sastri, J. H.; Abdu, M. A.; Batista, I. S.; Sobral, J. H. A. Onset Conditions of
458 Equatorial (Range) Spread-F at Fortaleza, Brazil, During the June Solstice. J.
459 Geophys. Res., 102(A11), 24013-24021, 1997.

460 Sobral, J. H. A. and Abdu, M. A. "Latitudinal Gradient in the Plasma Bubble
461 Zonal Velocities as Observed by Scanning 630nm Airglow Measurements".
462 J. Geophys. Res., 95(A6), 8253-8257, 1990.

463 Sobral, J. H. A. Vivian M. de Castilho, M. A. Abdu, Hisao Takahashi, I. Paulino,
464 Ulisses A. C. Gasparelo, Daniela C. S. Arruda, Matheus Mascarenhas, C. J.
465 Zamlutti, C. M. Denardini, Daiki Koga, A. F. de Medeiros, R. A. Buriti,
466 Midnight reversal of ionospheric plasma bubble eastward velocity to
467 westward velocity during geomagnetically quiettime: Climatology and its
468 model validation. /12/2010 Journal of Atmospheric and Solar-Terrestrial
469 Physics 73,1520–1528 10.1016/j.jastp.2010.11.031, 2011.

470 Uemoto J, Ono, T, Kumamoto A, Iizima M Statistical analysis of the ionization
471 ledge in the equatorial ionosphere observed from topside sounder satellites.

472 J. Atmos. Solar Terr. Phys., 68 (12), 1340-1351, DOI:
473 10.1016/j.jastp.2006.05.015, 2006.

474 Tsunoda, RT On equatorial spread F: Establishing a seeding hypothesis. J.
475 Geophys. Res., 115 Art. No. A12303, DOI: 10.1029/2010JA015564, 2010.

476 Zain AFM, Abdullah S, Homam MJ, Seman FC, Abdullah M, Ho YH
477 Observations of the F3-layer at equatorial region during 2005. J. Atmos.
478 Solar Terr. Phys., 70, 918–925, doi:10.1016/j.jastp.2007.12.002, 2008.

479 Zhao B, Wan W, Liu L, Igarashi K, Yumoto K, Ning B Ionospheric response to
480 the geomagnetic storm on 13–17 April 2006 in the West Pacific region. J.
481 Atmos. Solar Terr. Phys., 71, 88-100, doi:10.1016/j.jastp.2008.09.029, 2009.

482

483

484 Table 1. Details of the digital ionosondes (DI) and GPS sites used in the present
485 study.

Location (Symbol)	Instrument	Coordinates	Dip Latitude
Palmas (PAL)	GPS	10.2° S, 48.2° W	05.7° S
Brasília (BRA)	GPS	15.9° S, 47.9° W	11.7° S
Rio Paranaíba (RPA)	GPS	19.2° S, 46.1° W	15.8° S
Cachoeira Paulista (CP)	DI	22.7° S, 45.0° W	19.2° S
Rio de Janeiro (RIO)	GPS	22.8° S, 43.3° W	19.8° S
Ourinhos (ORI)	GPS	22.9° S, 49.9° W	16.7° S
S. J. dos Campos (SJC)	DI and GPS	23.2° S, 46.0° W	17.6° S

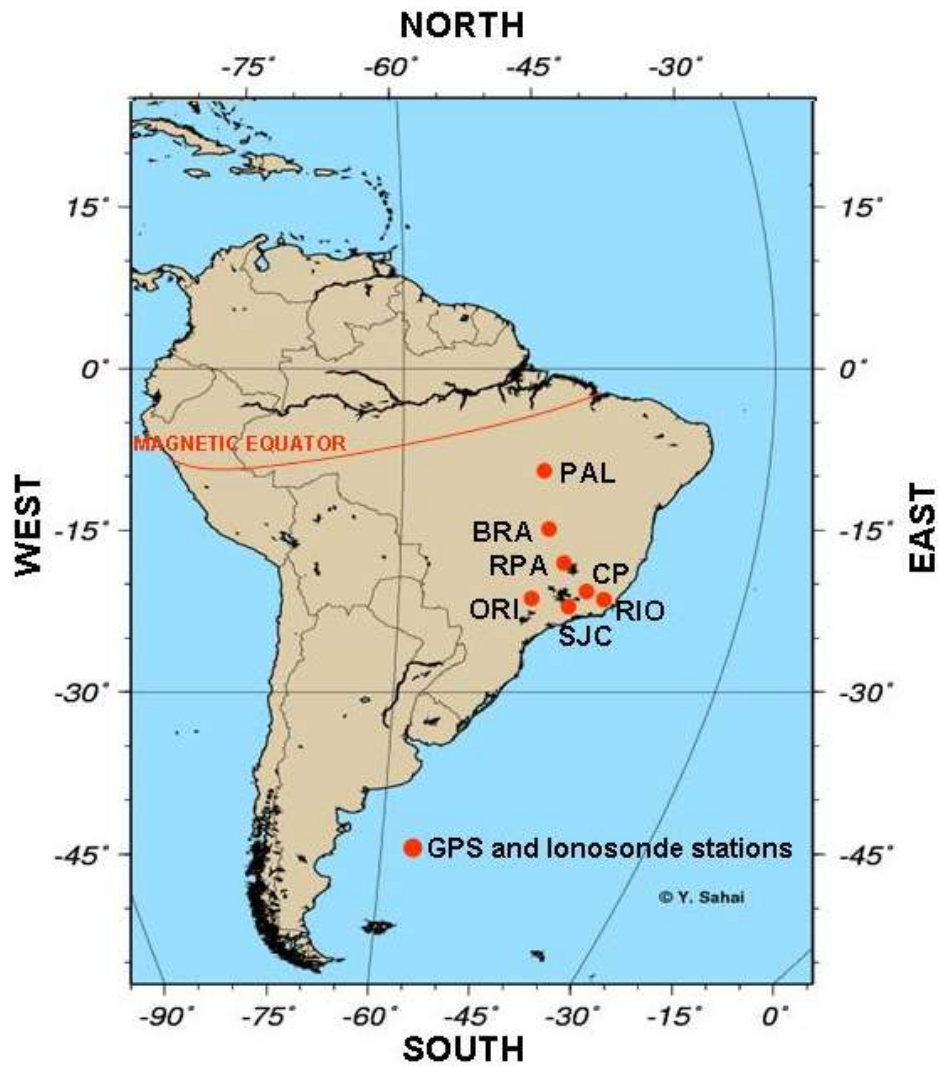
486

487

488

489

490

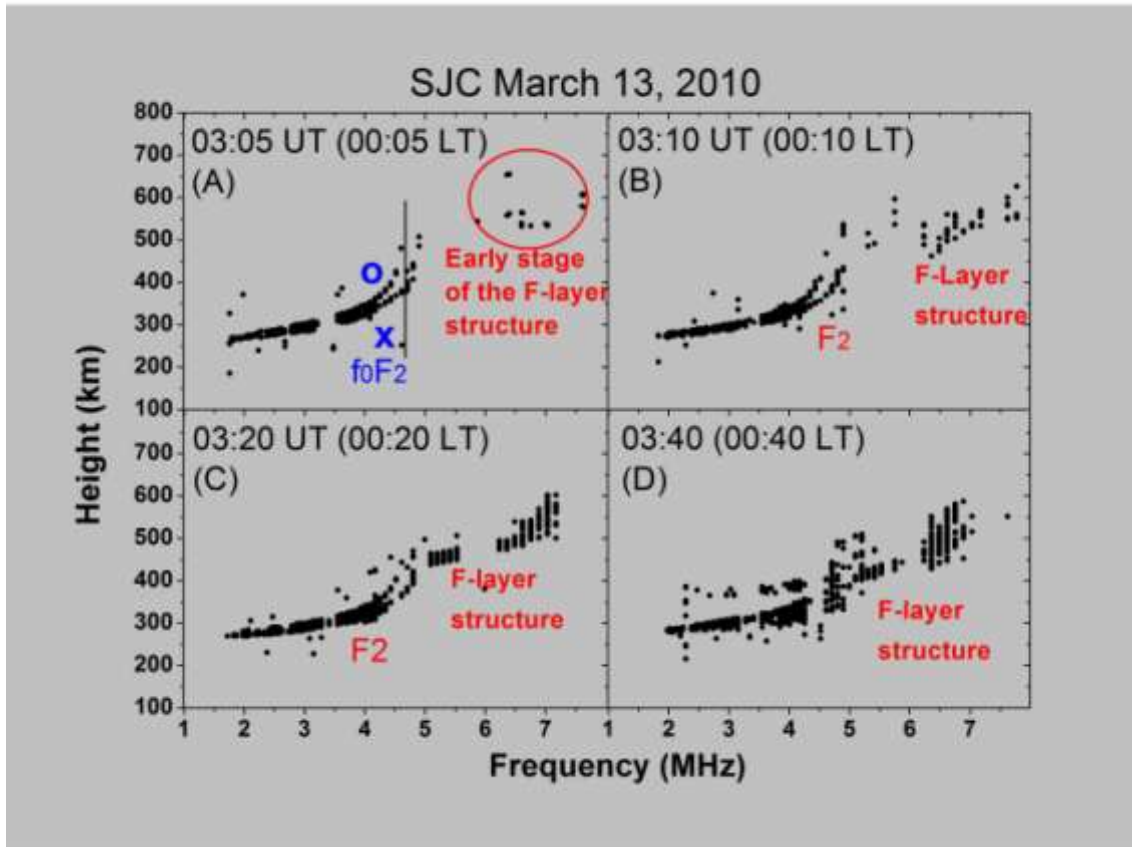


491

492 Figure 1. A map showing the locations of the digital ionosonde and GPS and
 493 stations used in the present study. Also, the geographic and magnetic
 494 equators are shown.

495

496



497

498 Figure 2. Ionograms obtained on March 13, 2010 for Sao Jose dos Campos

499 A) The early stage of spread-F traces structure formation; "O" and "X"

500 indicate the ordinary and extraordinary traces; critical frequency foF2=4.6

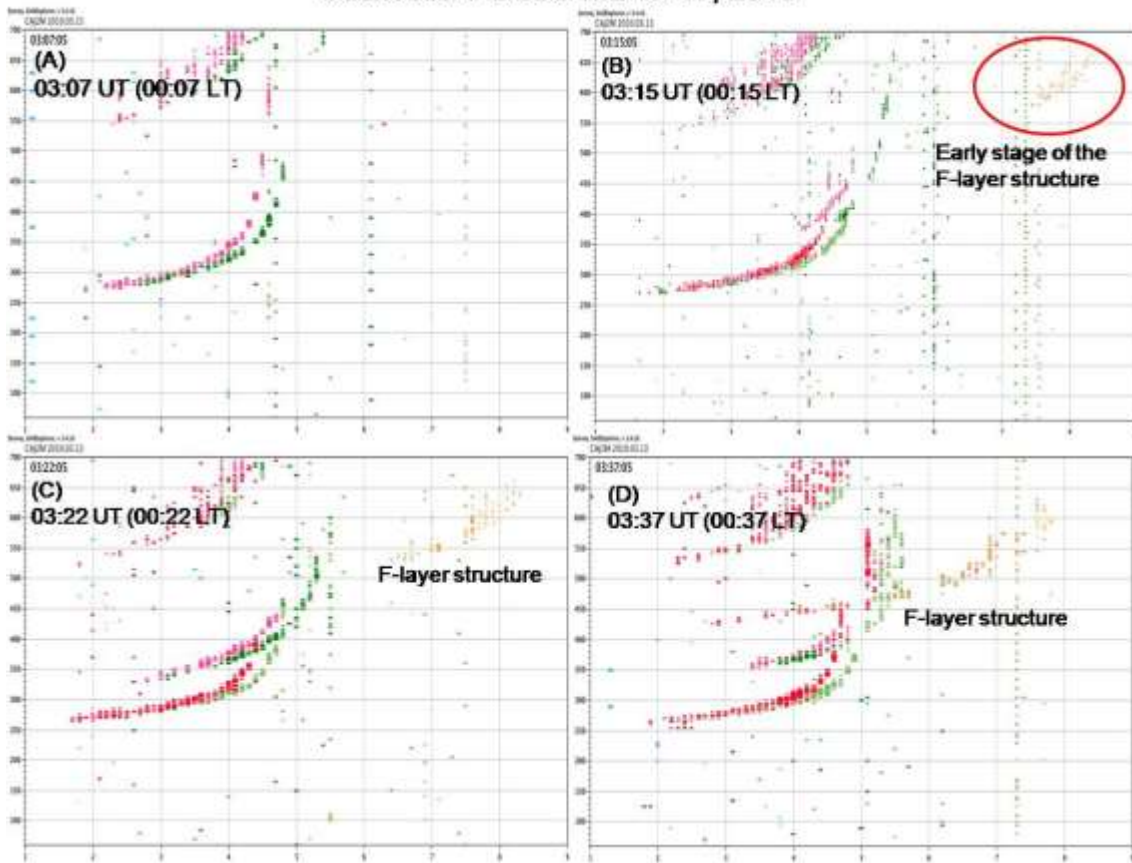
501 MHz. B) The spread-F traces structure became stronger. C) Spread-F traces

502 structure became a satellite trace to the F2-layer traces. D) The satellite

503 traces (spread-F traces structure) and the F2-layer traces are much closer.

504

Cachoeira Paulista March 13, 2010

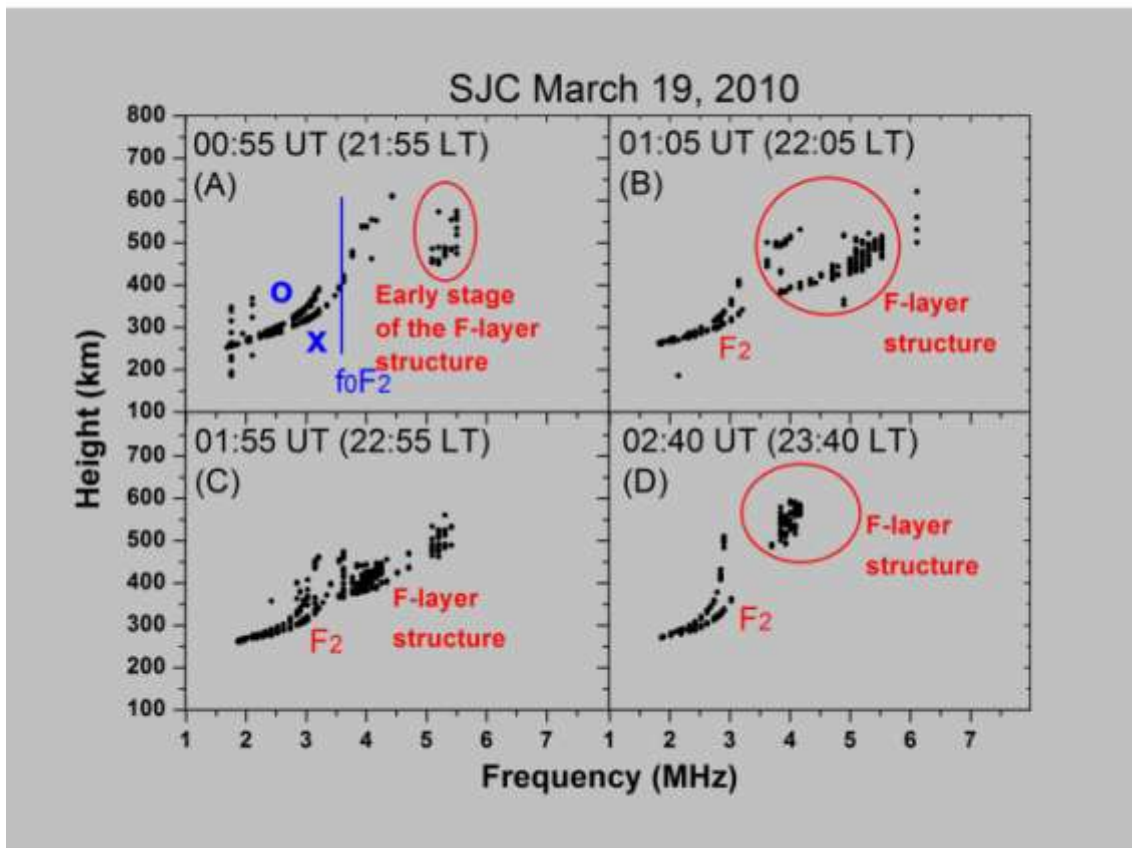


505

506 Figure 3. Ionograms obtained on March 13, 2010 for Cachoeira Paulista. A)
507 Ionogram just before the spread-F traces structure appears. B) The early stage
508 of spread-F traces structure formation. c) The spread-F traces structure
509 becomes stronger. D) Spread-F traces structure became satellite traces of the
510 F2-layer.

511

512



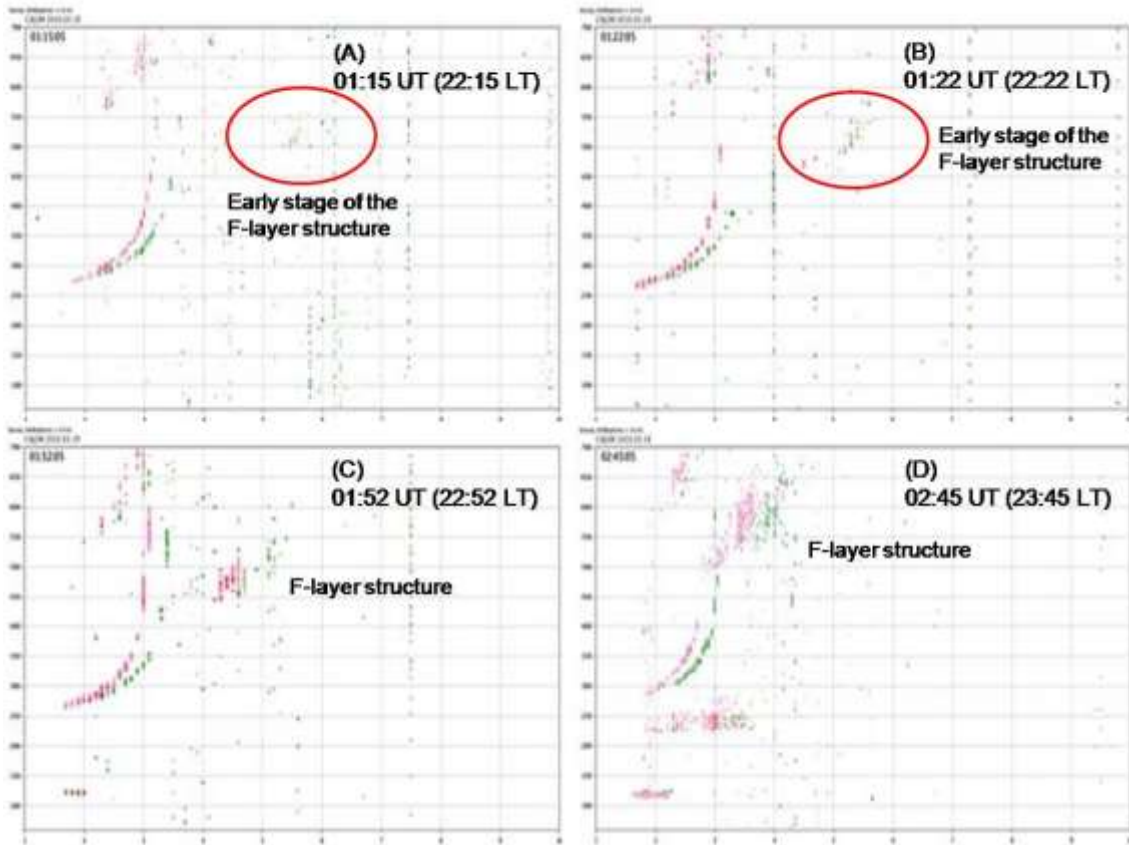
513

514 Figure 4. Ionograms obtained on March 19, 2010 for Sao Jose dos Campos A)
515 The early stage of F3 spread-F formation; "O" and "X" indicate the ordinary and
516 extraordinary traces; critical frequency foF2=3.5 MHz. B) The spread-F traces
517 became stronger. C) The spread-F traces structure became satellite traces of
518 the F2-layer traces. D) The spread-F traces get higher altitudes.

519

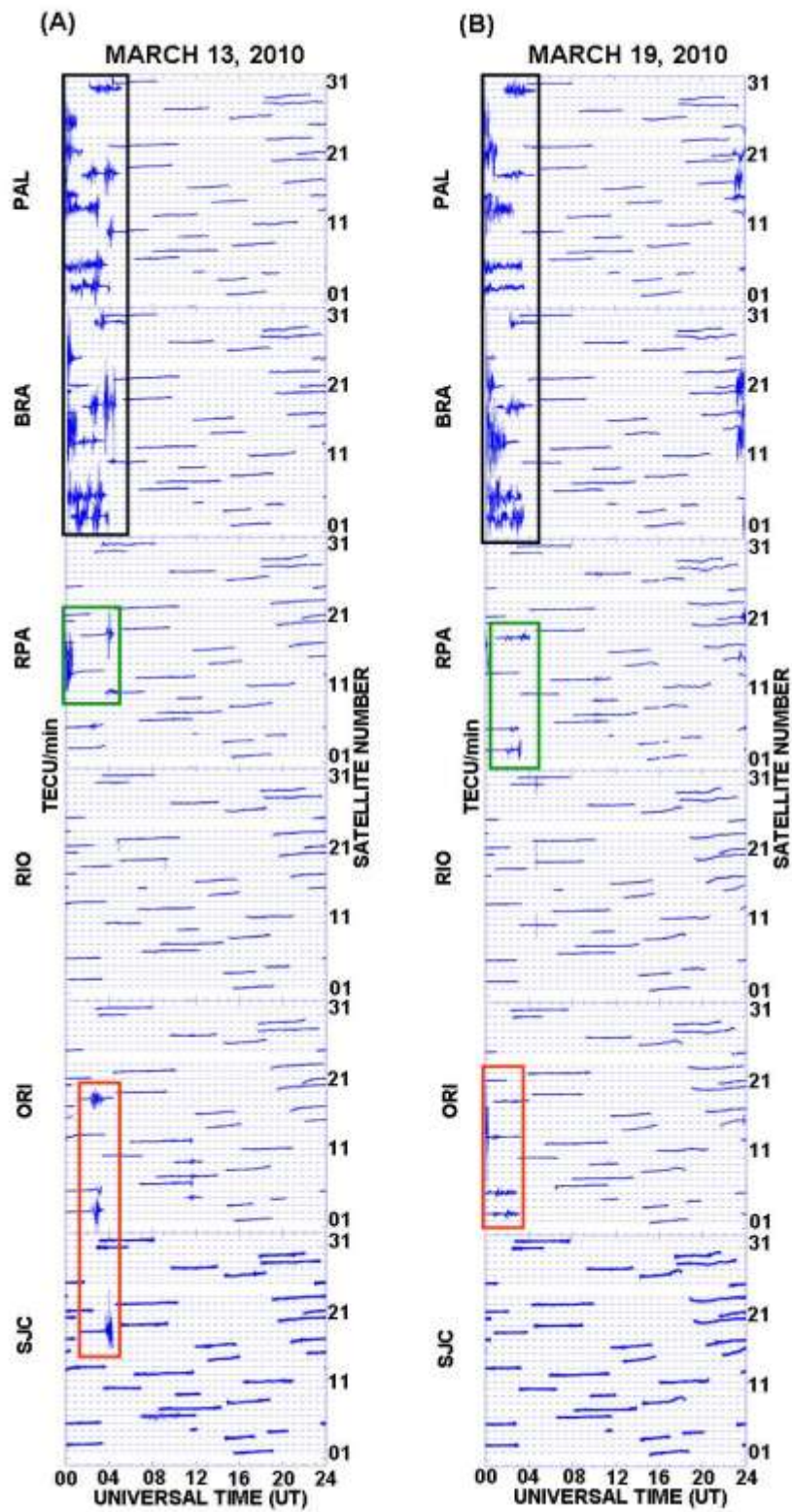
520

Cachoeira Paulista March 19, 2010



521

522 Figure 5. Ionograms obtained on March 19, 2010 for Cachoeira Paulista. A) The
523 early stage of spread-F traces structure formation. B) The early stage of spread-
524 F traces structure formation. C) The spread-F traces becomes stronger. D) The
525 spread-F traces structure get higher altitudes.



527 Figure 6- The phase fluctuations (ROT - rate of change of TEC) from GPS
528 observations obtained from different satellites at 6 receiving stations during the
529 period March 13 and 19, 2010.